Developmental Biology 349 (2011) 20–34

Contents lists available at ScienceDirect

Developmental Biology

journal homepage: www.elsevier.com/developmentalbiology

Fibroblast growth factor 10 represses premature cell differentiation during establishment of the intestinal progenitor niche

Pia Nyeng [a,*], Maureen Ann Bjerke [a], Gitte Anker Norgaard [a], Xiaoling Qu [b], Sune Kobberup [a], Jan Jensen [a,b]

[a] Barbara Davis Center for Childhood Diabetes, University of Colorado Health Sciences Center, 1775 N Ursula St. B140, 80045 Aurora, CO, USA
[b] Cleveland Clinic Foundation, Lerner Research Institute, Department of Stem Cell Biology and Regenerative Medicine, 9500 Euclid Avenue, Cleveland, 44195 OH, USA

ARTICLE INFO

Article history:
Received for publication 12 April 2010
Revised 29 August 2010
Accepted 20 September 2010
Available online 27 September 2010

Keywords:
Small intestine
FGF10
FGFR2
Differentiation
Progenitor
Mesenchymal–epithelial signaling

ABSTRACT

Spatio-temporal regulation of the balance between cell renewal and cell differentiation is of vital importance for embryonic development and adult homeostasis. Fibroblast growth factor signaling relayed from the mesenchyme to the epithelium is necessary for progenitor maintenance during organogenesis of most endoderm-derived organs, but it is still ambiguous whether the signal is exclusively mitogenic. Furthermore, the downstream mechanisms are largely unknown. In order to elucidate these questions we performed a complementary analysis of fibroblast growth factor 10 (*Fgf10*), gain-of-function and loss-of-function in the embryonic mouse duodenum, where the progenitor niche is clearly defined and differentiation proceeds in a spatially organized manner. In agreement with a role in progenitor maintenance, FGF10 is expressed in the duodenal mesenchyme during early development while the cognate receptor FGFR2b is expressed in the epithelial progenitor niche. *Fgf10* gain-of-function in the epithelium leads to spatial expansion of the progenitor niche and repression of cell differentiation, while loss-of-function results in premature cell differentiation and subsequent epithelial hypoplasia. We conclude that FGF10 mediated mesenchymal-to-epithelial signaling maintains the progenitor niche in the embryonic duodenum primarily by repressing cell differentiation, rather than through mitogenic signaling. Furthermore, we demonstrate that FGF10-signaling targets include ETS-family transcription factors, which have previously been shown to regulate epithelial maturation and tumor progression.

Introduction

Organogenesis is a fascinating developmental process involving a series of integrated events leading to the fully functional organ. Expansion of the committed progenitor cell population is an early event in organogenesis. This phase has received increasing attention during the past few years, due to the promising prospect of stem cell therapy, which has led to a need for knowledge on how to expand progenitor cells as a source for replacement therapy for multiple diseases. Likewise, balancing of progenitor cell expansion and differentiation features prominently in adult homeostasis of renewable organs, such as the intestine, and in the mutated state, also during cancer progression.

It is well known that reciprocal signaling between the epithelium and the surrounding mesenchyme via soluble and/or membrane-tethered signals is necessary for regulating growth and differentiation of the gut epithelium (Haffen et al., 1987;Kedinger et al., 1987), and several signaling pathways, including WNT (Korinek et al., 1998;Pinto et al., 2003), BMP (He et al., 2004), Notch (Fre et al., 2005;Jensen et al., 2000;van Es et al., 2005;Wong et al., 2004), and Hedgehog (Madison et al., 2005;Ramalho-Santos et al., 2000) have been implicated in regulating gastric and enteric development. Members of the fibroblast growth factor (FGF) family are mediators of mesenchymal-to-epithelial signaling in several organs, and are included as a component in many stem cell differentiation protocols. FGF10 in particular, has been shown to be necessary for progenitor maintenance during organogenesis of endoderm-derived organs, but it is still ambiguous whether the signal is exclusively mitogenic, or whether it also regulates cell differentiation. Furthermore, the downstream mechanisms are largely unknown.

Fgf10 is expressed in the mesenchyme of the embryonic duodenum (Bhushan et al., 2001;Kanard et al., 2005;Nyeng et al., 2007), as well as in the mesenchyme of the lung, stomach, pancreas, colon, and cecum (Bellusci et al., 1997;Burns et al., 2004;Fairbanks et al., 2004;Nyeng et al., 2007;Sala et al., 2006). Loss-of-function mutation of *Fgf10* or its cognate receptor *Fgfr2b* results in lung agenesis (Arman et al., 1999;Sekine et al., 1999), and severely affects the development of the glandular stomach (Spencer-Dene et al., 2006) and the pancreas (Bhushan et al., 2001; Pulkkinen et al., 2003). In the intestines, loss of *Fgf10* has been analyzed thoroughly in the colon (Sala et al., 2006) and the cecum (Burns et al.,

* Corresponding author. Present address: Lund University Stem Cell Center, BMC B10, Klinikgatan 26, 22184 Lund, Sweden.
E-mail addresses: Pia.Nyeng@med.lu.se (P. Nyeng), mabjerke@virginia.edu (M.A. Bjerke), gitte.noergaard@rh.dk (G.A. Norgaard), qux@ccf.org (X. Qu), skbb@hagedorn.dk (S. Kobberup), jensenj2@ccf.org (J. Jensen).

0012-1606/$ – see front matter © 2010 Elsevier Inc. All rights reserved.
doi:10.1016/j.ydbio.2010.09.010

2004), where attenuated proliferation and increased apoptosis led to colonic atresia and failure of cecal budding. Studies of clinical relevance have implicated *Fgf10* in intestinal pathobiology, as *Fgf10*−/− mice have duodenal (Kanard et al., 2005) and colonic (Fairbanks et al., 2005) atresia. Unfortunately, the duodenal phenotype was not analyzed further. So far, clinical studies have however failed to identify any association of mutations in *Fgf10* and duodenal atresia or anorectal malformations (Kruger et al., 2008;Tatekawa et al., 2007). The severe phenotype of loss of *Fgf10* prompted an analysis of *Fgf10* gain-of-function in order to understand the mechanism in more detail. Our studies of the stomach and pancreas have demonstrated that ectopic *Fgf10* overexpression in the epithelium results in inhibition of cell differentiation (Norgaard et al., 2003;Nyeng et al., 2007), a result that was corroborated by Hart et al in the pancreas (Hart et al., 2003). Quite likely, a central function of FGF-signaling in enteric progenitor maintenance has been overlooked, as previous studies focused mostly on the time after terminal differentiation. We therefore decided to study whether ectopic expression of *Fgf10* in the duodenal epithelium, disrupting the endogenous FGF10 gradient emanating from the mesenchyme, would suppress differentiation outside the progenitor niche, leading to an expansion of the niche. Reciprocally, we wished to test whether loss of *Fgf10* in the duodenum is sufficient to release progenitor cells and cause premature differentiation.

In the present work, we demonstrate that FGF10 mediated mesenchymal-to-epithelial signaling maintains the progenitor niche in the embryonic small intestine by repressing differentiation. Furthermore, we demonstrate that FGF10-signaling targets in the intestine include ETS-family transcription factors Etv4 and Etv5.

Materials and methods

Mouse derivation

Generation of a pPdx1-*Fgf10*^{FLAG} construct and derivation of transgenic mouse (*Mus musculus*) embryos, as described earlier (Norgaard et al., 2003), were approved by the UCHSC Animal Care and Use Committee. A total of 3 embryonic day 12.5 (E12.5) and 6 E18.5 pPdx1-*Fgf10*^{FLAG} embryos and their wildtype (WT) littermates were obtained by oocyte injection using FVB mice. The day of oocyte transfer was counted as embryonic day 0.5 (E0.5). BrdU (20 mg/kg) was injected 2 h prior to isolation of embryos. Targeted disruption of *Fgf10* has already been described (Min et al., 1998). A total of 8 E14.5 and 8 E18.5 *Fgf10*−/− embryos were obtained by timed mating of heterozygotes which had been outbred on a CD1 background. The day of vaginal plug was counted as E0.5. Heterozygotic littermates were used as controls throughout, as they were indistinguishable from wildtype embryos.

All embryos were genotyped by PCR. *pPdx1-Fgf10*^{FLAG} embryos were genotyped using *Fgf10-Flag* primers (Table S1) and *Fgf10*−/− embryos were genotyped using *Fgf10* KO P1, P2, P3 and P4 primers as described (Sekine et al., 1999). Expression of the *pPdx1-Fgf10*^{FLAG} construct was confirmed by RT-PCR of three E18.5 embryos and WT littermates. *pPdx1-Fgf10*^{FLAG} embryos varied somewhat in their expression of the transgene, but although phenotypes were not identical, they were highly similar, and the phenotypic variation never exceeded that observed in *Fgf10*−/− mice.

Tissue and RNA isolation

Whole guts were dissected in ice-cold PBS and fixed in 4% PFA overnight. They were then immersed in 30% sucrose for at least 4 h, in 1:1 30% sucrose and OCT embedding medium for 1 h and finally in OCT for 1 h before embedding. Tissue blocks were freeze sectioned at a thickness of 6 μm using a cryotome. Embryos for RNA analysis were dissected in ice-cold PBS and the upper half of the duodenum including mesenchyme and epithelium was extracted using the RNeasy (Qiagen) kit including a DNAse treatment step. Endogenous *Fgf* expression was analyzed using RNA from embryos from time-mated CD1 mice. RNA from E12.5 whole small intestine was pooled from 5 embryos for each sample. Whole duodenal tissue was pooled from 4 E14.5 embryos, 3 E15.5 embryos or 2 embryos for each of the samples at E16.5, E17.5 and E18.5. At least three samples were analyzed per time point.

Multiplex RT-PCR analysis

Purified total RNA was analyzed by a semi-quantitative low-cycle radioactive multiplex RT-PCR (MPX-RT-PCR) method previously described (Jensen et al., 1996) with 2 μg of total RNA per sample. A primer set for the TATA box binding protein (Tbp) or Alpha-tubulin (α-tubulin) was included in all reactions as an internal control and used for standardization. Primers (Supplementary Material Table S1) were specifically designed for MPX-RT-PCR, optimized for exponential amplification within the cycle range and tested for interference. Six primers were included in each reaction and the reaction was carried out at 96 °C for 1 min, followed by 28 cycles of 96 °C for 30 s, 55 °C for 30 s and 73 °C for 30 s. Following the RT-PCR reaction, samples were run on a denaturing sequencing gel. The gel was subsequently exposed to phosphoimage storage screen for 3 days, after which the screen was scanned. Experiments were carried out in triplicate for each sample and values are expressed as mean ± SEM relative to *Tbp* or *α-tubulin*.

Immunohistochemistry

Immunohistochemistry (IHC) was carried out as already described (Norgaard et al., 2003). Primary antibodies are included in Table S1. 0.1% Triton X-100 was added to the blocking buffer. After overnight incubation with the primary antibodies, slides were washed and incubated with rabbit/goat/rat/mouse/guinea pig secondary antibody conjugated to Texas red/Cy2/AMCA (Jackson ImmunoResearch, PA, USA) for 1 h or taken through the Histostain kit protocol (Zymed/Invitrogen, CA, USA), followed by tyramide signal amplification (TSA) (Perkin Elmer, MA, USA) as indicated in Table S1. Nuclei were stained with Hoechst dye for morphometric studies. Mature goblet cells were stained for 1 h using rhodamine-conjugated Dolichos biflorus agglutinin (DBA), while immature goblet cells were stained with fluorescein conjugated Bauhinia purpurea lectin/agglutinin (BPA). Apoptotic cells were detected using a TUNEL kit (DeadEnd Fluorometric TUNEL System, Promega, WI, USA) according to protocol.

In situ hybridization

Digoxygenin labeled RNA in situ probes where synthesized and in situ hybridization (ISH) of tissue sections carried out as in (Norgaard et al., 2003) from purified restriction fragments obtained from sequence-validated plasmids listed in Supplementary Material Table S1.

Histochemistry

Harris hematoxylin and eosin Y staining was carried out according to standard protocols.

Goblet cells were stained for morphometry using Alcian blue/Periodic Acid Schiff (PAS). Frozen slides were thawed and stained 15 min with Alcian Blue (Newcomersupply, WI, USA). After washing, the slides were covered with periodic acid (Sigma-Aldrich, MO, USA) for 5 min, rinsed and stained with Schiffs reagent for 6 min (Sigma-Aldrich). Finally, slides were washed and nuclei stained with Gills hematoxylin (Sigma-Aldrich).

Image analysis

Images were obtained in ImagePro v. 4.5 (Media Cybernetics, MD, USA) using a Pixera CL600 camera, mounted on an Olympus BX51 microscope station equipped with differential interference contrast.

All analysis was performed on at least three cryosections from each of three E18.5 pPdx1-*Fgf10*^{FLAG} and three wildtype littermates or four E18.5/E14.5 *Fgf10*−/− and four heterozygous littermates for each age. The sections were distributed equally across the duodenum. For morphometric analysis, digital images of a maximum of ten non-overlapping fields of view were quantified per slide in ImagePro. Total epithelial area was measured using area integration based on E-cadherin immunostaining. The total number of epithelial cells was automatically counted by the software based on Hoechst and E-cadherin staining after application of the limited watershed algorithm. Specialized cell types were counted manually based on immunostaining, with exception of goblet cells which were quantified based on Alcian blue/PAS staining.

Results

Fgf10 and Fgfr2b are expressed complementarily in the duodenal mesenchyme and epithelium

In order to verify that FGF10 and FGFR2b mediate mesenchymal–epithelial signaling in the duodenum we first performed an expression analysis of the two isoforms of *Fgfr2* as well as the known FGFR2b ligands Fgf1, Fgf3, Fgf7 and Fgf10 in whole duodenum during development. mRNA analysis showed that while expression of *Fgf1* increased during development and *Fgf3* and *Fgf7* levels where negligible, *Fgf10* expression was highest at E14.5 before initiation of terminal differentiation (Fig. 1A, B), in accordance with a role in progenitor maintenance. Both isoforms of *Fgfr2* where expressed in the duodenum at a constant level throughout development taking into account the internal control (Fig. 1B). We proceeded to analyze the spatial expression pattern of *Fgf10* and *Fgfr2b* in more detail. In situ hybridization (ISH) confirmed that *Fgf10* is highly expressed in the stomach and intestine at E14.5 (Fig. 1C), with strongest expression in the mesenchyme (Fig. 1C'). At E18.5, when *Fgf10* levels are lower, expression is mainly confined to smooth muscle (Fig. 1D). Using the Bek antibody which detects both splice forms of FGFR2 we observed expression primarily in the epithelium at E14.5 and E18.5. At E18.5, expression was limited to the intervillus epithelium, where the progenitor niche is located (Fig. 1E, F). Analysis of *Fgfr2b*−/− tissue using the Bek antibody confirmed that only FGFR2b is expressed in the intestinal epithelium, while FGFR2c is mesenchymal, as epithelial staining was absent (results not shown). High *Fgf10* expression in the

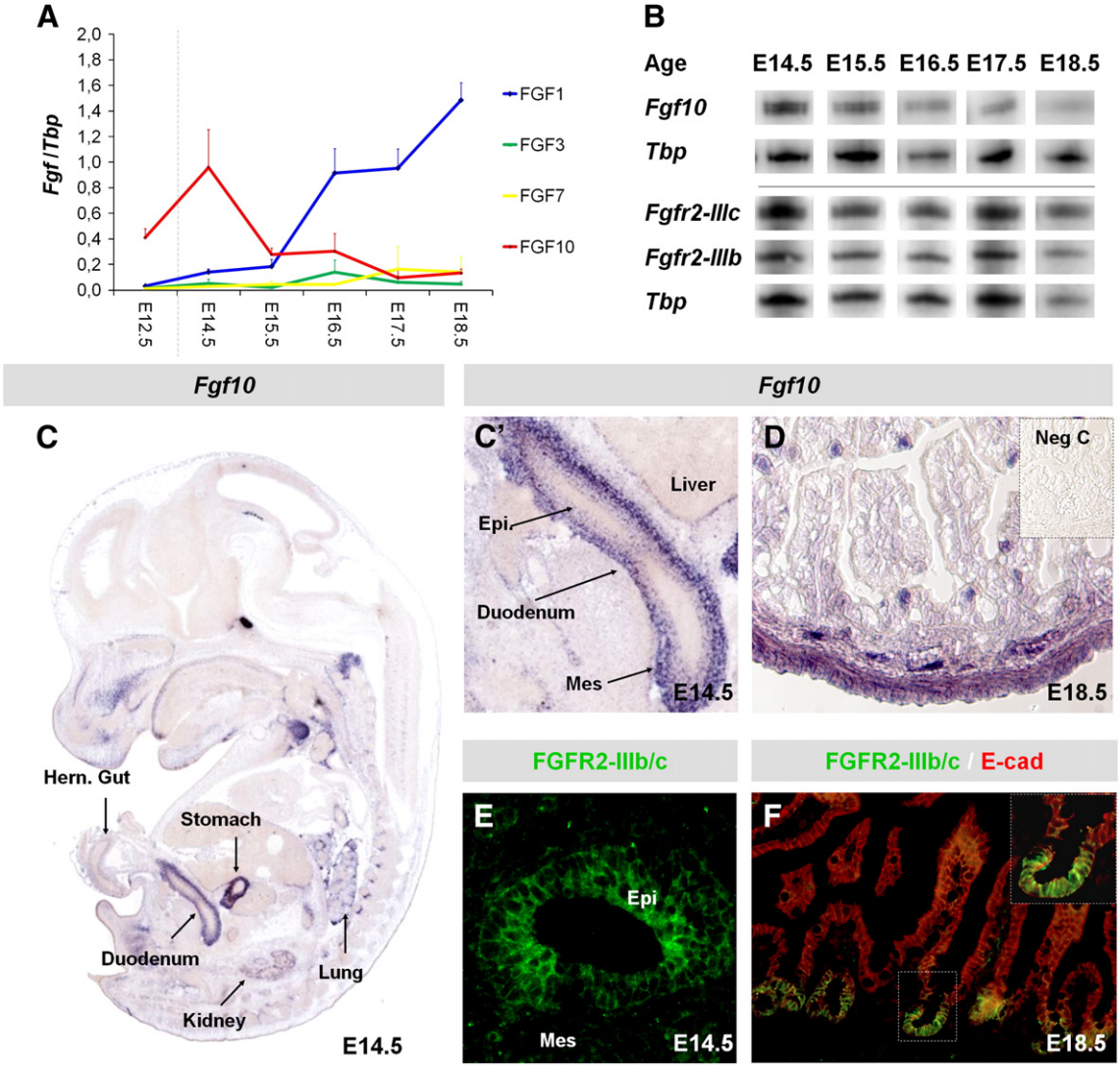

Fig. 1. Fibroblast growth factor expression in the developing duodenum. A: MPX-RT-PCR analysis of *Fgf1*, *Fgf3*, *Fgf7*, and *Fgf10* expression in E12.5 small intestine and E14.5-E18.5 duodenum. Dotted line indicates that E12.5 small intestine samples are not directly comparable with duodenum samples. $N = 3$ per age. Graph depicts band volume intensity as a fraction of *Tbp* intensity. B: Representative MPX-RT-PCR bands for *Fgf10*, *FgfR2-IIIc*, *FgfR2-IIIb* and *Tbp*. $N = 3$ per age. C: ISH of E14.5 embryo (From Genepaint (Visel et al., 2004)) with *Fgf10* probe. C': Magnification of duodenum from C. D: *Fgf10* ISH of E18.5 duodenum. E and F: IHC for FGFR2 using an antibody that detects both isoforms. Duodenum from E14.5 (E) and E18.5 (F) with E-cadherin counterstain in F. Mes: mesenchyme, Epi: epithelium.

duodenum before terminal differentiation and confinement of *Fgfr2b* expression to the progenitor niche makes it plausible that FGF10 has a role in duodenal progenitor maintenance, similarly to what has been observed in other endodermal organs.

Fgf10 overexpression interferes with epithelial morphogenesis and disrupts the crypt–villus axis

To test whether *Fgf10* overexpression in the epithelium itself can trigger expansion of the duodenal progenitor pool, we analyzed *pPdx1-Fgf10^{FLAG}* embryos, which express *Fgf10* in the *Pdx1* domain (Norgaard et al., 2003;Nyeng et al., 2007). *Pdx1* is expressed in epithelium of the posterior stomach, anterior duodenum and the pancreatic anlagen from their initial specification at E8.5 (Ohlsson et al., 1993) and continues to be expressed in the duodenum throughout development and into adulthood (Boyer et al., 2006;Nyeng et al., 2007).

In order to verify expression of the transgene, mRNA and protein expression analyses were carried out using low sensitivity assays that do not detect endogenous levels of *Fgf10*. At E12.5, exogenous *Fgf10* mRNA and protein were mosaically expressed in the uniform epithelium (Supplemental Material Fig. S1). At E18.5, exogenous *Fgf10* mRNA expression was confined to the basal intervillus region, as would be expected based on the *Pdx1* expression domain. However, FGF10 protein as detected with FGF10 or FLAG antibodies was also expressed outside the intervillus region at this time, as the basement membrane was conditioned with FGF10/FLAG along the greater part of the villus. We therefore conclude that the transgene is expressed in the basal domain of the duodenum, but that the protein is found along the entire crypt–villus axis, most likely due to secretion and cell membrane adherence.

As *pPdx1-Fgf10^{FLAG}* mice die at birth, each embryo was obtained by oocyte injection and represents a separate integration event. As a result transgene expression levels varied somewhat between embryos (Supplemental Material Fig. S1K), but although not identical, phenotypes were highly similar.

Histological analysis revealed a striking phenotype manifested after terminal differentiation. At E12.5, when the duodenal epithelium normally forms a multilayered cylinder of uniformly PDX1 and FGFR2 expressing cells (Fig. 2A), the *pPdx1-Fgf10^{FLAG}* epithelium already displayed some defects in morphogenesis. The epithelium was irregular in places, consisting of multilayered as well as monolayered regions of cells with variable PDX1 expression (Fig. 2B), but unchanged FGFR2 expression (insert in Fig. 2B). These changes were not confined to regions with FGF10^{FLAG} expressing cells. At E18.5, villus morphogenesis was aberrant with pronounced branching (arborization) (Fig. 2D and H&E staining in Supplementary Material Fig. S2B). The epithelial cells were however properly polarized on the villi with lateral expression of β-catenin (Fig. 2C–G). One exception was seen in ectopic branch nodes (arrows in Fig. 2D), where cells were unpolarized (Fig. 2H). These branch nodes were only found in transgenic tissue and were strongly PDX1 positive (Fig. 2H), although PDX1 is normally confined to the basal intervillus region (Fig. 2E and G). FGFR2 expression had also expanded outside the basal region (Fig. 2I–L) and *FgfR2*b was upregulated in all embryos analyzed (Fig. 2Q), suggesting an expansion of the basal population into the villus domain. In order to confirm an expansion of the basal niche we analyzed expression of the basal markers *Cdx2* and

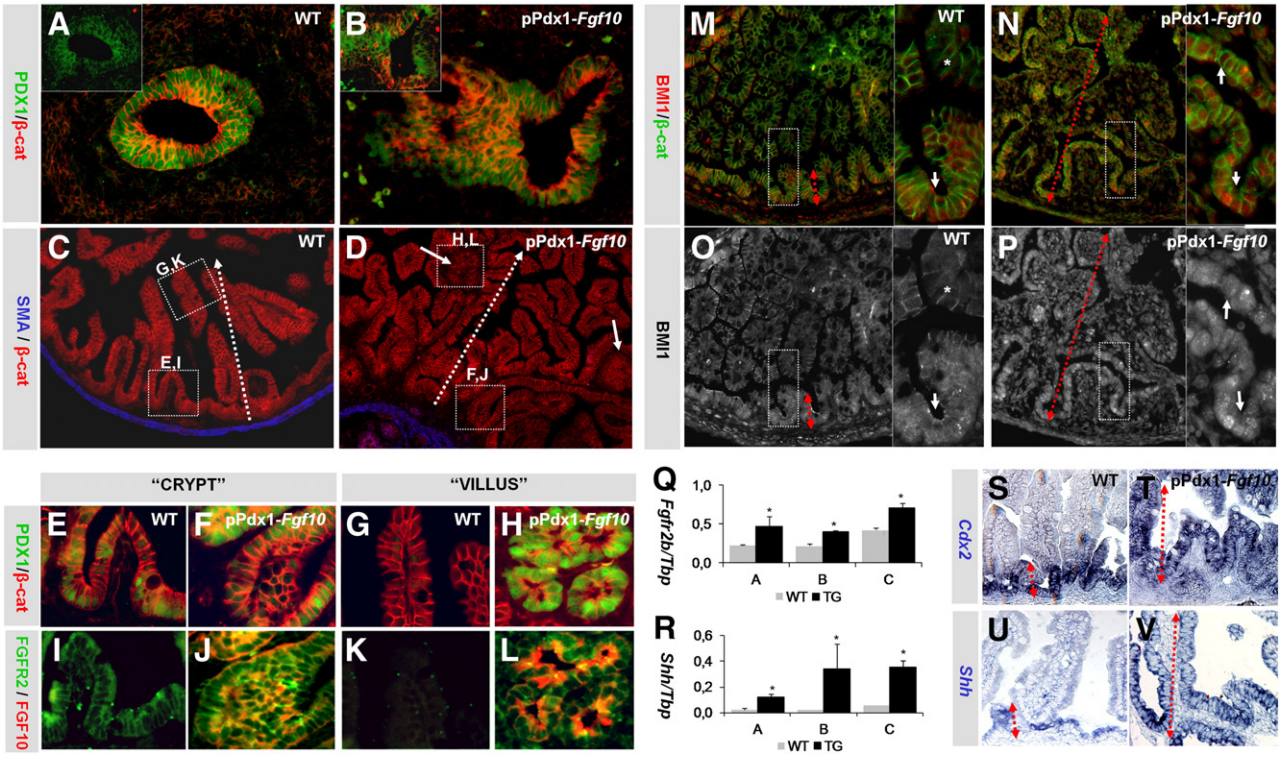

Fig. 2. Disturbed duodenal morphogenesis. A–B: PDX1 and β-catenin IHC of E12.5 WT (A) and *pPdx1-Fgf10^{FLAG}* (B) duodenum. Picture inserts: FGFR2 and FGF10 IHC on adjacent sections. C–D: SMA and β-catenin IHC of E18.5 WT (C) and *pPdx1-Fgf10^{FLAG}* (D) duodenum. Note the two ectopic branch points in D (solid arrows). The stippled arrows indicate the crypt–villus axis. Boxed areas are further analyzed in E–L below. E-H: PDX1 and β-catenin IHC of villi and crypt regions as outlined in C and D. I–L: FGFR2 and FGF10 IHC of villi and crypt regions as outlined in C and D (adjacent section). Note how PDX1 and FGFR2 are upregulated in the villus region of transgenic tissue. M–P: BMI1 and β-catenin IHC of E18.5 WT (M and O) and *pPdx1-Fgf10^{FLAG}* (N and P) duodenum. In the WT, BMI1 is expressed exclusively in the intervillus domain (arrows in insert M and O) with no expression on the villus (asterisk), while BMI1 expression is seen throughout the epithelium in the *pPdx1-Fgf10^{FLAG}* tissue (arrows in insert N and P). Q: *Fgfr2b* expression in whole E18.5 duodenum as measured by MPX-RT-PCR of WT and *pPdx1-Fgf10^{FLAG}* (TG) tissue. R: *Shh* expression in whole E18.5 duodenum as measured by MPX-RT-PCR of WT and *pPdx1-Fgf10^{FLAG}* (TG) tissue. S–T: ISH of *Cdx2* on WT (S) and *pPdx1-Fgf10^{FLAG}* (T) duodenum. P: U–V: ISH of *Shh* on WT (U) and *pPdx1-Fgf10^{FLAG}* (V) duodenum. Red stippled arrows demarcate the expression domains. MPX-RT-PCR graphs depict band volume intensity as a fraction of Tbp intensity for each of three embryos (A, B and C). Mean values of $n = 3$ experiments plus SEM. *p-Value calculated using Student's t-test < 0.05.

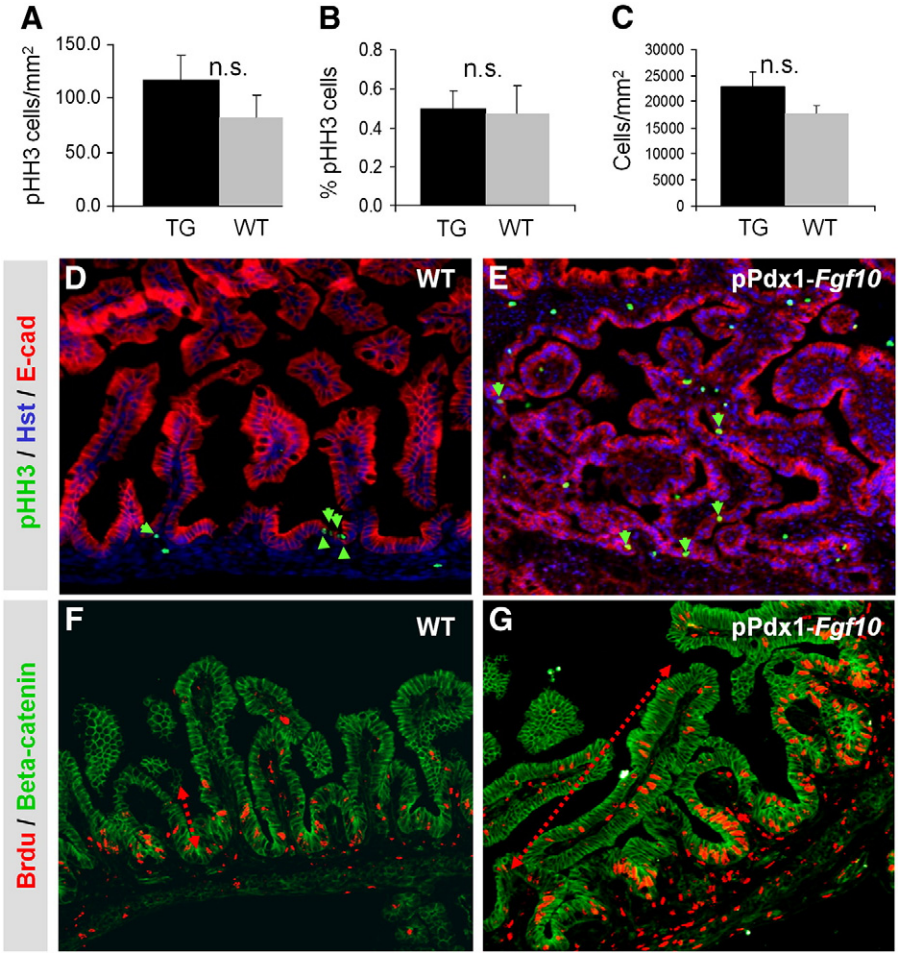

Fig. 3. The proliferative zone is disrupted while proliferative index remains unchanged. A–C: Mean values of $n = 3$ plus SEM. p-Value as calculated using Student's T-test were >0.5 (n.s.: not significant). A: pHH3$^+$ cells per mm^2 epithelial area (E-cadherin$^+$). B: Percent pHH3$^+$ cells per total number of epithelial cells (E-cadherin$^+$, Hoechst$^+$). C: Total number of epithelial cells per epithelial area. There is no significant difference in any of the parameters. D–E: pHH3, Hoechst and E-cadherin IHC. Arrowheads point to epithelial pHH3$^+$ cells. F–G: BrdU and β-Catenin IHC showing expansion of the proliferative niche (red arrow).

Shh, showing expansion of the *Cdx2* and *Shh* positive population into the villus domain and upregulation of *Shh* (Fig. 2R–V). We also analyzed expression of the adult enteric stem cell marker BMI1 (Sangiorgi and Capecchi, 2008), and found a marked expansion of BMI1 expressing cells from the intervillus region to the entire epithelium (Fig. 2M–P) We conclude that increased presence of FGF10 in duodenum leads to a complete failure in establishment of a spatially restricted progenitor niche. Since the progenitor niche with proliferating cells is normally already confined to the basal intervillus region at E18.5, we next questioned whether cell cycle control would also be affected by FGF10.

Failure to confine a proliferative niche in the presence of high FGF10 levels does not impact the proliferative index

A clear disruption of the proliferative niche was evident at E18.5: Proliferating cells positive for phospho-Histone H3 (pHH3) (Fig. 3D and E) or BrdU (Fig. 3F and G) were distributed throughout the villus in the *pPdx1-Fgf10^{FLAG}* duodenum as opposed to a strict confinement of proliferating cells to the basal intervillus region in wildtype littermates. Since the proliferative niche is the seat of the progenitor cells, these results provide further evidence that ectopic expression of FGF10 caused expansion of the progenitor niche. Surprisingly, this expansion was not correlated with an increase in proliferative index in the epithelium, as pHH3 positive cells per epithelial area or as a percentage of epithelial cells was unaltered (Fig. 3A and B). Mean cell size (Fig. 3C) as well as apoptosis rate (data not shown) was also unchanged, precluding that these parameters caused the observed changes. The number of pHH3 positive cells per area was also unchanged in the mesenchyme (*pPdx1-Fgf10*: 41cells/mm^2 ± 9. WT: 51 cells/mm^2 ± 20, $p = 0.6$). Expansion of the progenitor niche is therefore most likely due to failure of cells to exit the progenitor pool through terminal differentiation.

FGF10 overexpression causes a global attenuation of cell maturation

The intestinal Paneth cells, goblet cells, enteroendocrine cells and absorptive enterocytes derive from a common enteric progenitor. Although the enteric cells are not fully mature until after birth, they can be distinguished prenatally based on cell-specific expression. In situ hybridization for *Cryptdin-1 (Defa1)* (Desai et al., 2008) and multiplex RT-PCR for *Cryptdin-6* (*Defa6*) demonstrated a complete absence of these cryptdins in E18.5 *pPdx1-Fgf10^{FLAG}* duodenum, at a time when wildtype littermates have an abundance of Paneth cell

Fig. 4. Attenuation of terminal cell fates. A, B: ISH for *Cryptdin3*$^+$ Paneth cells. C, D: ISH for *Fabp2*$^+$ enterocytes. E, F: *Tff3* ISH for goblet cells. G–I: IHC with Dolichos biflorus agglutinin (DBA) and Bauhinia purpurea agglutinin (BPA). G: WT. Insert shows DBA^{POS} BPA^{NEG} cell. H: *pPdx1-Fgf10^{FLAG}*. Insert shows DBA^{NEG} BPA^{POS} cell and a double positive cell. I: WT colon. Insert shows basally located BPA^{POS} cells. J: Morphometry based on Alcian Blue/PAS staining. Mean values of $n = 3$ plus SEM. p-Values were calculated using Student's t-test. ns: not significant.

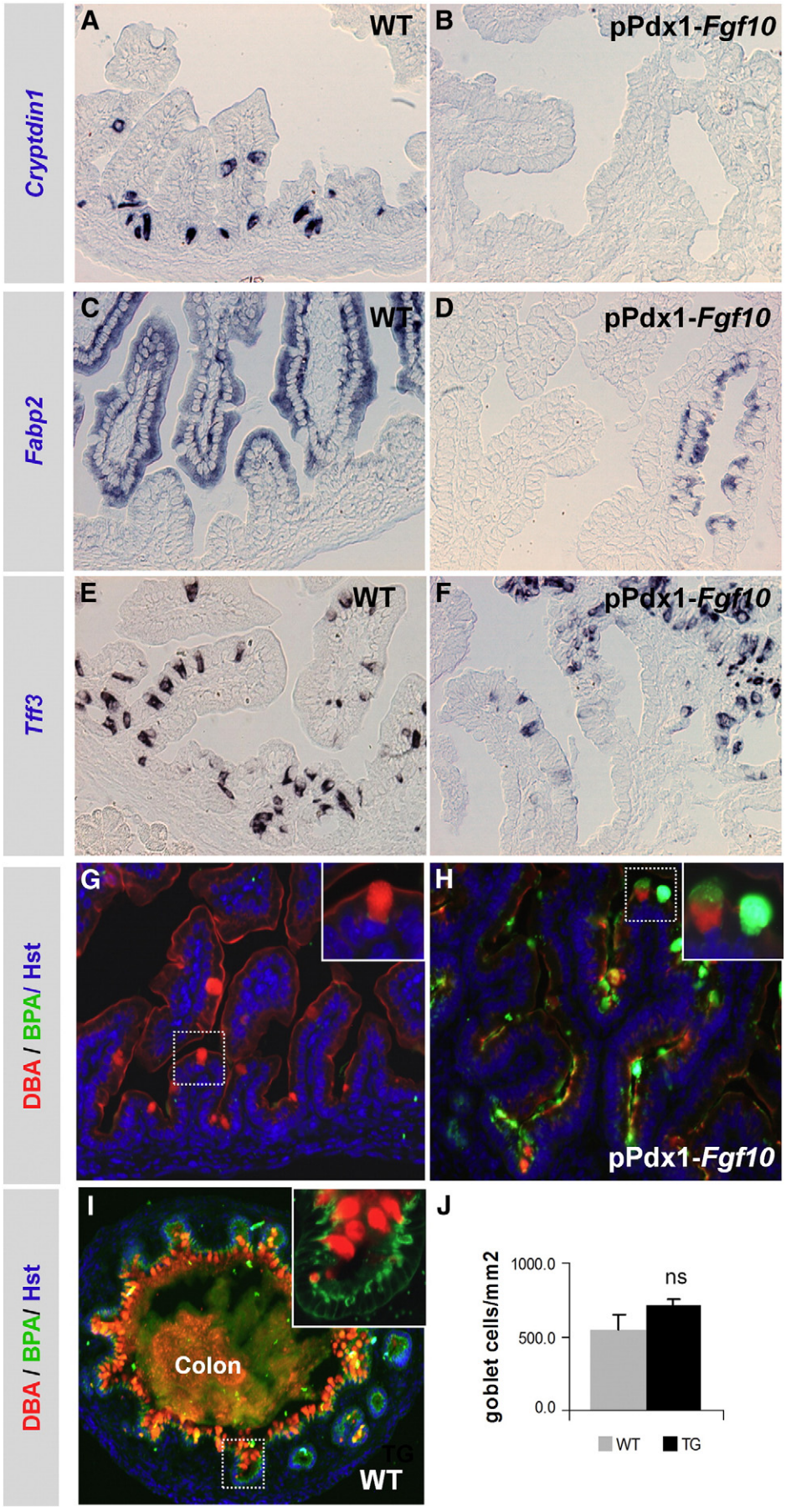
Cryptdin1
A
WT
B
pPdx1-Fgf10
Fabp2
C
WT
D
pPdx1-Fgf10
Tff3
E
WT
F
pPdx1-Fgf10
DBA / BPA/ Hst
G
H
pPdx1-Fgf10
DBA / BPA/ Hst
I
Colon
TG
WT
J
goblet cells/mm2
1000.0
500.0
0.0
ns
WT
TG

precursors expressing *Cryptdin-1* and *Cryptdin-6* mRNA (Fig. 4A–B and Supplementary Material Fig. S3A). Likewise, in situ hybridization and multiplex RT-PCR for *Fabp2* revealed that the number of absorptive enterocytes was greatly diminished by the ectopic expression of *Fgf10* (Fig. 4C–D and Supplementary Material Fig. S3B). Conversely, Trefoil factor 3 (*Tff3*) mRNA analysis (Fig. 4E–F and Supplementary Material Fig. S3C) as well as staining with alcian blue or alcian blue/PAS (results not shown) showed that goblet cells were still present in comparable numbers to wildtype. This was confirmed by morphometric analysis of alcian blue/PAS positive cells (Fig. 4J). However, goblet cells in transgenic mice displayed a significantly lowered reactivity for Dolichos Biflorus Agglutin (DBA, Fig. 4G–H), which is only present in mature goblet cells (Boland et al., 1982; Wurster et al., 1983), and instead reacted with Bauhinia Purpurea Agglutinin (BPA). Goblet cells that did bind DBA also bound BPA in most cases (See insert in Fig. 4H). This was never observed in the WT duodenum. BPA preferentially labels less differentiated mucin in human goblet cells found at the bottom of crypts (Boland et al., 1982). We confirmed that this is also the case in the mouse (Fig. 4I), where BPA was confined to crypt cells while DBA was found further up along the radial axis in the colon (see insert in Fig. 4I). We conclude that goblet cell maturation is arrested at an immature state by *Fgf10* overexpression. Enteroendocrine cells, as detected using the pan-endocrine marker Chromogranin A (ChrgA), were reduced by more than half (57% reduction, $^*p<0.05$, Fig. 5A). Morphometric analysis for the various enteroendocrine cell types revealed that this overall decrease was due to a marked reduction in secretin producing enterochromaffin cells (40% reduction, $^*p<0.05$) and somatostatin producing D cells (56% reduction, $^*p<0.05$). The mean of both the GIP (44% reduction, $p=0.19$) and serotonin (48% decrease, $p=0.15$) positive cells in *pPdx1-Fgf10*^{FLAG} duodenum were not significantly changed, although all transgenic embryos had lower cell numbers than wildtype littermates. We ascribe this to a pronounced litter-specific variation among both wildtype and transgenic embryos (see error bars in Fig. 5A). The occurrence of CCK and ghrelin producing cells was unchanged, showing that these enteroendocrine cell fates remain irresponsive to FGF10. In conclusion, a global attenuation, but not complete inhibition, of cell differentiation could be ascertained. We therefore asked whether a specific attenuation of early precursor cells was occurring.

Growth factor independent 1 (GFI1) is a zinc finger transcription factor important for regulating Paneth/goblet versus enteroendocrine cell fate (Shroyer et al., 2005). GFI1 is expressed in the secretory cell progenitor and in endocrine cells (Fig. 5F, G). Since immature goblet cells still formed while endocrine cell differentiation was attenuated, we tested whether this could be due to direct changes in GFI1. Fewer

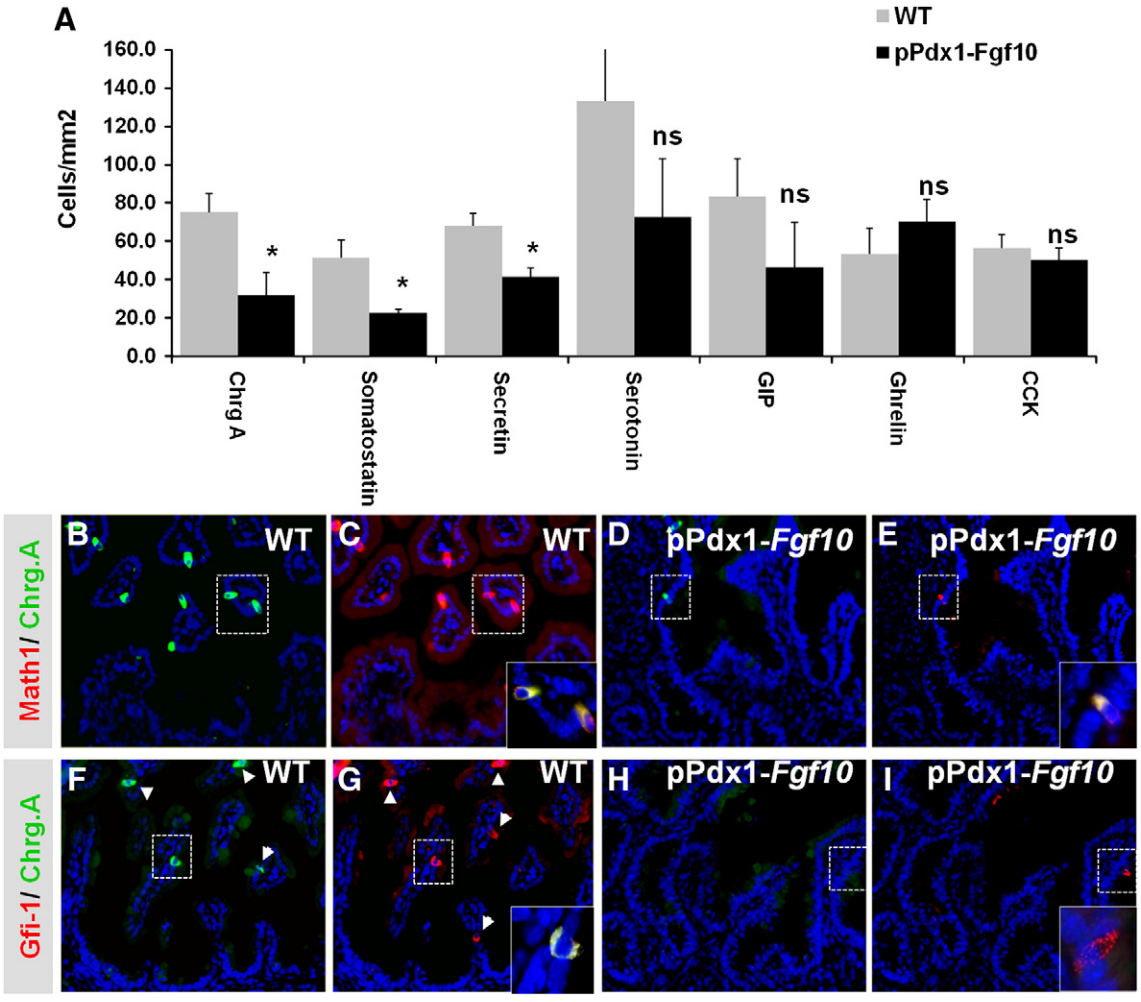

Fig. 5. Endocrine cell differentiation. A: Morphometric analysis of endocrine cell types in *pPdx1-Fgf10*^{FLAG} and WT littermate E18.5 embryos from three different litters ($n=3$). Values were calculated as the mean number of positive cells per epithelial area plus SEM based on co-staining of E-cadherin and ChrgA/somatostatin/serotonin/secretin/GIP/ghrelin/CCK. Ns: not significant. $^*p<0.5$. B–E: IHC of MATH1 and ChrgA with Hoechst. B: ChrgA in WT duodenum. C: MATH1 in WT. Insert shows MATH1/ChrgA co-localization. D: ChrgA in *pPdx1-Fgf10*^{FLAG} duodenum. E: MATH1 in *pPdx1-Fgf10*^{FLAG}. Insert shows MATH1/ChrgA co-localization. F: ChrgA expression in WT duodenum. F: GFI1 in WT. Insert shows GFI1/ChrgA co-localization. H: ChrgA expression in *pPdx1-Fgf10*^{FLAG} duodenum. I: GFI1 in *pPdx1-Fgf10*^{FLAG}. Insert shows no co-localization. Arrowheads indicate positive cells.

GFI1$^+$ cells were present in the transgenic epithelium (Fig. 5H–I). While GFI1 co-localized with ChrgA in most wildtype cells (Fig. 5F–G), the few GFI1$^+$ cells found in the *pPdx1-Fgf10^{FLAG}* duodenum were ChrgA negative (Fig. 5H–I). Atonal homolog 1 (*Atoh1/Math1*), which is upstream from GFI-1 and is necessary for differentiation of all enteric secretory cells (Yang et al., 2001), was also much decreased in *pPdx1-Fgf10^{FLAG}* duodenum (Fig. 5D–E). Most of the remaining Math1$^+$ cells co-localized with ChrgA (Fig. 5E), representing the few endocrine cells that formed. MATH1 single-positive goblet cell precursors were found in very few cases (data not shown), demonstrating that the inhibiting effect of FGF10 is acting on the common secretory precursor cells as well as the absorptive enterocyte cell lineage, but that the few precursor cells that do form, preferentially enter the goblet cell lineage.

Overexpression of FGF10 leads to upregulation of ETS-factors

In order to elucidate the downstream effects of ectopic FGF10 overexpression, we analyzed expression of downstream target of FGF-signaling in three *pPdx1-Fgf10^{FLAG}* embryos (designated A, B and C). *Sprouty2* (*Spry2*), a FGF-induced feedback inhibitor (Minowada et al., 1999), was upregulated in transgenic duodenum (Fig. 6A) confirming that transgenic *Fgf10* activates FGF-signaling. The ETS-factors *Etv5* (*Erm*) and *Etv4* (*Pea3*) are targets of the MAP-kinase pathway and have been shown by our group to mediate FGF10 downstream effects in the pancreas (Kobberup et al., 2007), and probably has a similar function in the lung (Liu et al., 2003). *Etv5* and *Etv4* were significantly upregulated in all three embryos compared to littermate controls (Figs. 6B-C). IHC for ETV4 further demonstrated that expression was upregulated and that this was due to an expansion of the expression domain from the progenitor niche to the villus epithelium (Fig. 6D–E). *Fgf10* overexpression thus caused transcriptional upregulation of ETS-factor targets of the MAP-kinase pathway.

We did not find any changes in Wnt and BMP signaling (Supplementary Material Fig. S4), and although we did see a transcriptional decrease in the Notch ligand Delta1, we failed to find changes in Notch, Jagged and Hes1 expression (Supplementary Material Fig. S4 and results not shown).

Loss of Fgf10 results in epithelial hypoplasia

Given that gain-of-function of *Fgf10* leads to attenuation of cell differentiation and expansion of the progenitor niche, we questioned using a loss-of-function model whether *Fgf10* is required for suppression of differentiation in the progenitor population. A preliminary inspection of E14.5 *Fgf10*−/− embryos revealed minor alterations of the duodenum, which was slightly thinner and in some cases had a bend between anterior and posterior duodenum (Fig. 7A, asterisk). At E18.5 the duodenum was noticeably smaller and duodenal atresia and swelling was observed in some embryos (Fig. 7B), as already reported (Kanard et al., 2005). E18.5 *Fgf10*−/− embryos were divided into three classes: no duodenal atresia, incomplete atresia (Type I) and complete atresia (Type II). Although embryos with no atresia also had pronounced duodenal defects, including a decrease in villus length and villus differentiation defects, only type I and type II embryos were analyzed in detail in the following.

Villus formation is normally initiated shortly before E14.5 by the formation of epithelial elevations. In *Fgf10*−/− embryos this process was delayed, as protrusions were either lacking or subnumerary compared to wildtype (Fig. 7C–D). This reflected in a lack of villi in the anterior-most duodenum and stunted villi in the mid duodenum at E18.5; a phenotype that was more pronounced in type II atresia (Fig. 7I–K). The posterior duodenum appeared unaffected by the loss of *Fgf10* (data not shown).

Changes in the proliferative and apoptotic indices do not suffice to account for epithelial hypoplasia

The observed hypoplasia of the duodenum could be due to decreased proliferation, increased apoptosis or loss of progenitor cells through premature or excessive differentiation. No difference in proliferative activity was seen in the epithelium at E14.5 (Fig. 7C–G), and contrarily to what has been observed in other organs, loss of *Fgf10* led to a relative increase in proliferating cells per epithelial area at E18.5 (Fig. 7H and L–Q). The proliferating cells were located in the basal position of progenitor cells, and their absolute number was unchanged. The relative increase in cell proliferation could thus be

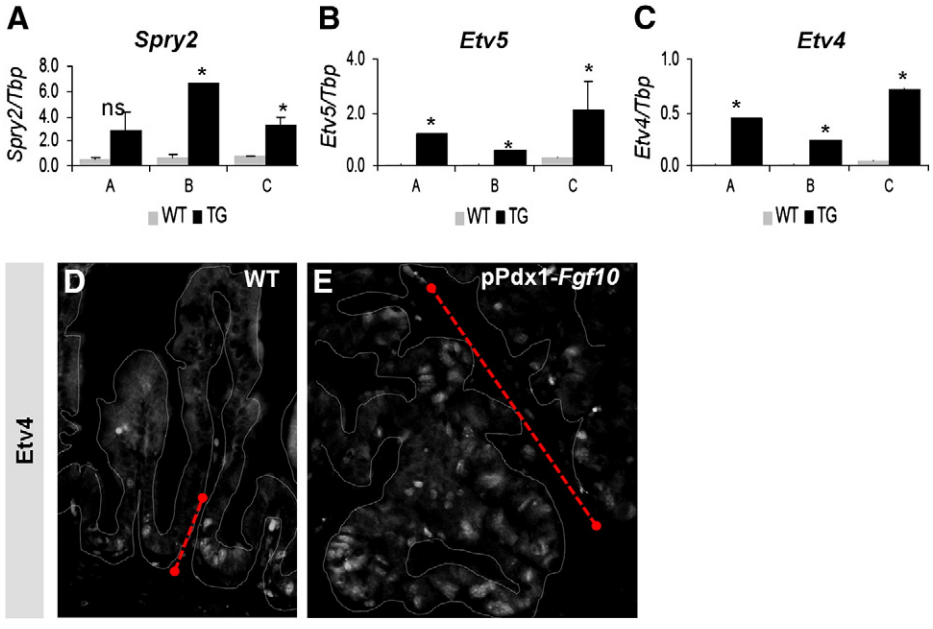

Fig. 6. Increased FGF10 levels leads to upregulation of SPRY and ETS-factor expression. A–C: MPX-RT-PCR analysis of mRNA expression. Mean values plus SEM from three experiments are shown relative to *Tbp* expression. *p*-Values were calculated using Student's *t*-test. $^*p<0.5$, ns: not significant. A: *Spry2*, B: *Etv5*, C: *Etv4*. D: ETV4 IHC on E18.5 WT and *pPdx1-Fgf10^{FLAG}* duodenum. Arrow shows extent of Etv4 expression. Stippled line outlines the epithelium.

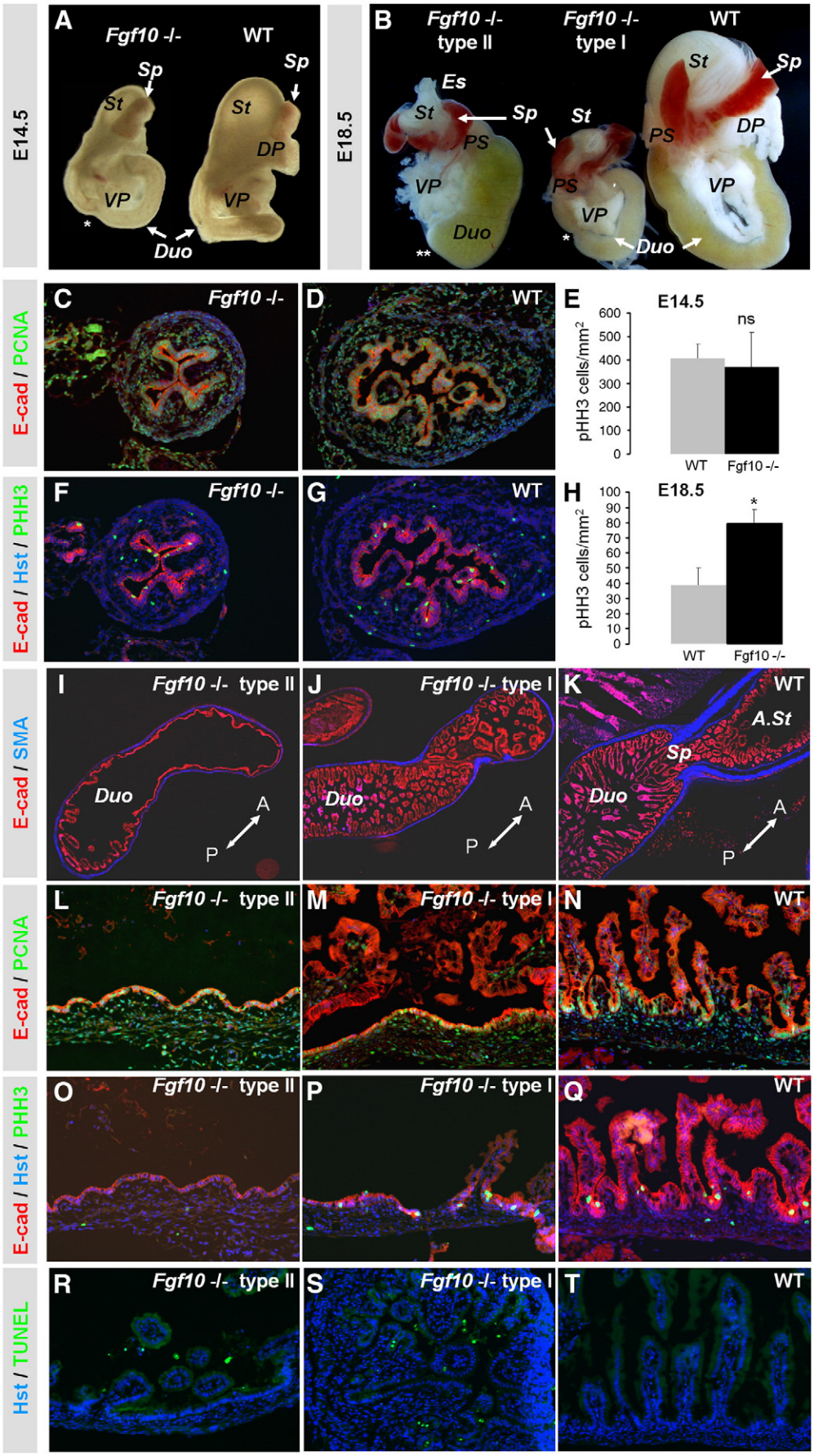
E14.5
E18.5
A
Fgf10 -/-
WT
Sp
St
DP
VP
Duo
B
Fgf10 -/- type II
Fgf10 -/- type I
Es
PS
E-cad / PCNA
E-cad / Hst / PHH3
C
D
E
E14.5
ns
pHH3 cells/mm2
WT
Fgf10 -/-
F
G
H
E18.5
E-cad / SMA
I
J
K
A.St
A
P
L
M
N
O
P
Q
Hst / TUNEL
R
S
T

ascribed to loss of villus epithelium. A TUNEL analysis demonstrated increased cell death at E18.5 (Fig. 7R–T), but not at E14.5 (results not shown). Strikingly, the majority of the apoptotic cells had been shed from the villus into the lumen, a process thought to occur by anoikis. Cell shedding is normally not observed in the embryonic duodenum, as it constitutes the departure of mature enterocytes from the constantly regenerating adult epithelium. The presence of shed cells in the embryonic duodenum could therefore indicate a maturation defect. As the changes in proliferation and apoptosis were furthermore insufficient to account for the observed hypoplasia we next proceeded to analyze differentiation.

Fgf10 is necessary for suppression of premature differentiation

Enteric differentiation normally starts at E16.5. However, when analyzing cell differentiation in E14.5 *Fgf10*−/− duodenum several ChrgA$^+$ endocrine cells (Fig. 8A, D), *Cryptdin3*$^+$ Paneth cells (Fig. 8F) and *Fabp2*$^+$ absorptive enterocytes (Fig. 8H), and an increased number of *Tff3*$^+$ cells (Fig. 8J) were found, signifying that loss of *Fgf10* results in premature differentiation of all enteric cell lineages. Surprisingly, many *Tff3*$^+$ pre-goblet cells (Fig. 8I) were found in the WT duodenum already at E14.5, indicating that this cell lineage starts forming earlier than was previously thought.

We expected to see a loss of differentiated cells at E18.5 similarly to what has been observed in the pancreas (Bhushan et al., 2001) as a consequence of the overall loss of progenitor cells to premature differentiation. Attesting to the great regenerating potential of the intestinal epithelium, most enteric cell types were however present at proportionally normal levels when analyzed at E18.5 (Supplementary Fig. S5), with exception of enterocytes (*Fabp2*$^+$) and enterochromaffin cells (secretin$^+$), which were greatly decreased.

In order to determine if the observed premature cell differentiation was associated with a decrease in factors needed for stem cell and/or progenitor maintenance, we analyzed for changes in BMI1, nuclear beta-catenin and HES1. In agreement with our results from the gain-of-function model, we did not observe any changes in HES1 (Supplementary Fig. S5). BMI1 is widely expressed in the nuclei of embryonic cells at E14.5 (Fig. 9A and C). In the absence of FGF10 we did however observe patches of BMI1 negative cells located on epithelial ridges (Fig. 9B and D). These BMI1 negative cells also did not express beta-catenin in the nucleus, when analyzed with an antibody that can detect both nuclear and membrane bound beta-catenin (Fig. 9E–F).

We conclude that the epithelial hypoplasia observed in the duodenum of *Fgf10*−/− embryos is primarily the effect of loss of progenitor cells by premature differentiation at E14.5.

Discussion

The intestinal epithelium is an excellent model for studies of the transition from progenitor maintenance to cell differentiation, as it allows us to study this transition in both time and space. During embryogenesis, the intestinal epithelium goes through a temporal transition from a uniform epithelium consisting exclusively of progenitor cells to an epithelium consisting of both progenitors and differentiated cells. Furthermore, a spatial transition also takes place, as the crypt–villus unit is established with stem cells and progenitor cells located in the basal region and differentiated cells located primarily on the villus (see Fig. 10). This study provides evidence that mesenchymal secretion of FGF10 is necessary for stem and progenitor cell maintenance in the duodenum through suppression of premature differentiation, leading to severe defects in loss and gain-of-function models.

FGF10 is expressed by the mesenchyme at high levels at E14.5 and decreases hereafter, but is still present before birth, while FGFR2b is expressed in basally located epithelial cells. This expression pattern makes the ligand–receptor pair a likely candidate for regulation of enteric progenitor cells both before and after establishment of the crypt–villus unit. Previous studies based on loss-of-function models have shown that FGF10 and/or FGFR2b signaling is necessary for expansion and survival of the enteric progenitor population (Burns et al., 2004; Sala et al., 2006), while studies of gain-of-function models in other endodermal organs have suggested that FGF10 primarily is required for maintenance of the progenitor population through inhibition of differentiation (Hart et al., 2003;Norgaard et al., 2003; Nyeng et al., 2007). In this study we therefore undertook to compare gain-of-function and loss-of-function of *Fgf10* in the duodenum. Using a *pPdx1-Fgf10*^{FLAG} construct we ectopically overexpressed *Fgf10* in the duodenal epithelium, in order to abolish the normal FGF10 gradient. *Fgf10*^{FLAG} mRNA expression was mosaic at E12.5 and confined to the crypt areas at E18.5. Similar to endogenous mesenchymal FGF10, the transgenic FGF10 protein was secreted and could therefore be found throughout the epithelium at E18.5. This secretion made *Fgf10*^{FLAG} available to the entire duodenal epithelium, and effects of the transgene were seen throughout the radial axis. The *pPdx1-Fgf10*^{FLAG} model thus likely involves both autocrine signaling in the FGF10^{FLAG} and FGFR2b expressing epithelial cells and paracrine signaling from the aforementioned cells to neighboring epithelial and mesenchymal cells. Co-expression of FGF-receptor and ligand leading to autocrine FGF-signaling is not as unusual as one could assume, and has been observed in for example muscle cells (Miyamoto et al., 1998), embryonic stem cells (Dvorak et al., 2005) and many cancers (Powers et al., 2000), and we therefore find it likely that autocrine signaling is also taking place in the *pPdx1-Fgf10*^{FLAG} model. Although the mesenchyme does not express FGFR2b, it expresses low levels of the FGFR2c isoform, which also binds FGF10, although with a significantly lower specificity compared to FGFR2b (Zhang et al., 2006)). We therefore cannot exclude that some effects are mediated through the mesenchyme.

At E18.5, the duodenal epithelium is in the process of forming crypt–villus units, and radial patterning has already led to a niche specific localization of progenitor and stem cells. Ectopic overexpression of *Fgf10* causes a disruption of the polarization of the crypt–villus axis due to expansion of the progenitor/stem cell niche, with expression of basal markers PDX1, FGFR2, *Cdx2* and *Shh* expanded along the entire villus axis. The stem cell marker BMI1 is confined to a few cells located at position +4 near the bottom of adult crypts (Sangiorgi and Capecchi, 2008). We here show that BMI1 is also confined to a small cell population in the forming crypt at E18.5, but is expanded throughout the entire epithelium in the *pPdx1-Fgf10*^{FLAG} model.

Also, dividing cells were distributed throughout the villus, while overall apoptotic and proliferative indices were unchanged. These

Fig. 7. *Fgf10* loss leads to duodenal atresia and epithelial hypoplasia. A: E14.5 *Fgf10*−/− and WT guts. All *Fgf10*−/− stomachs were considerably smaller than WT. Notice bend in proximal duodenum (*). B: E18.5 *Fgf10*−/− and WT guts. Duodenal circumference and length was decreased except where swollen as a result of complete atresia. **Site of complete atresia (type II). *Site of incomplete atresia (type I). C–D: E-cadherin, PCNA and Hoechst IHC of E14.5 *Fgf10*−/− (C) and WT (D) proximal duodenum. E: Quantification of pHH3 positive cells per epithelial area (mm^2) plus SEM. There is no significant difference (ns) between WT and *Fgf10*−/− E14.5 proximal duodenum. F–G: E-cadherin, pHH3 and Hoechst IHC of E14.5 *Fgf10*−/− (F) and WT (G) proximal duodenum. H: Quantification of pHH3 positive cells per epithelial area (mm^2) plus SEM. E18.5 *Fgf10*−/− proximal duodenum has a significantly higher proliferative index compared to WT (*$p<0.05$). I–K: SMA and E-cadherin IHC at E18.5. I: KO with complete atresia and duodenal swelling. J: KO with incomplete atresia. K: WT. Anterior to posterior axis is shown in each picture (A<->P). L–N: E-cadherin, PCNA and Hoechst IHC of E18.5 *Fgf10*−/− type II (L), type I (M) and WT (N) proximal duodenum. O–Q: E-cadherin, pHH3 and Hoechst IHC of E18.5 *Fgf10*−/− type II (O), type I (P) and WT (Q) proximal duodenum. R–T: TUNEL and Hoechst staining of E18.5 *Fgf10*−/− type II (R), type I (S) and WT (T) proximal duodenum. There was no detectable epithelial apoptosis in any of the WT embryos examined. Es: esophagus, St: stomach, VP: ventral pancreas, DP: dorsal pancreas, Sp: sphincter, Duo: duodenum. A. St: Antral stomach region.

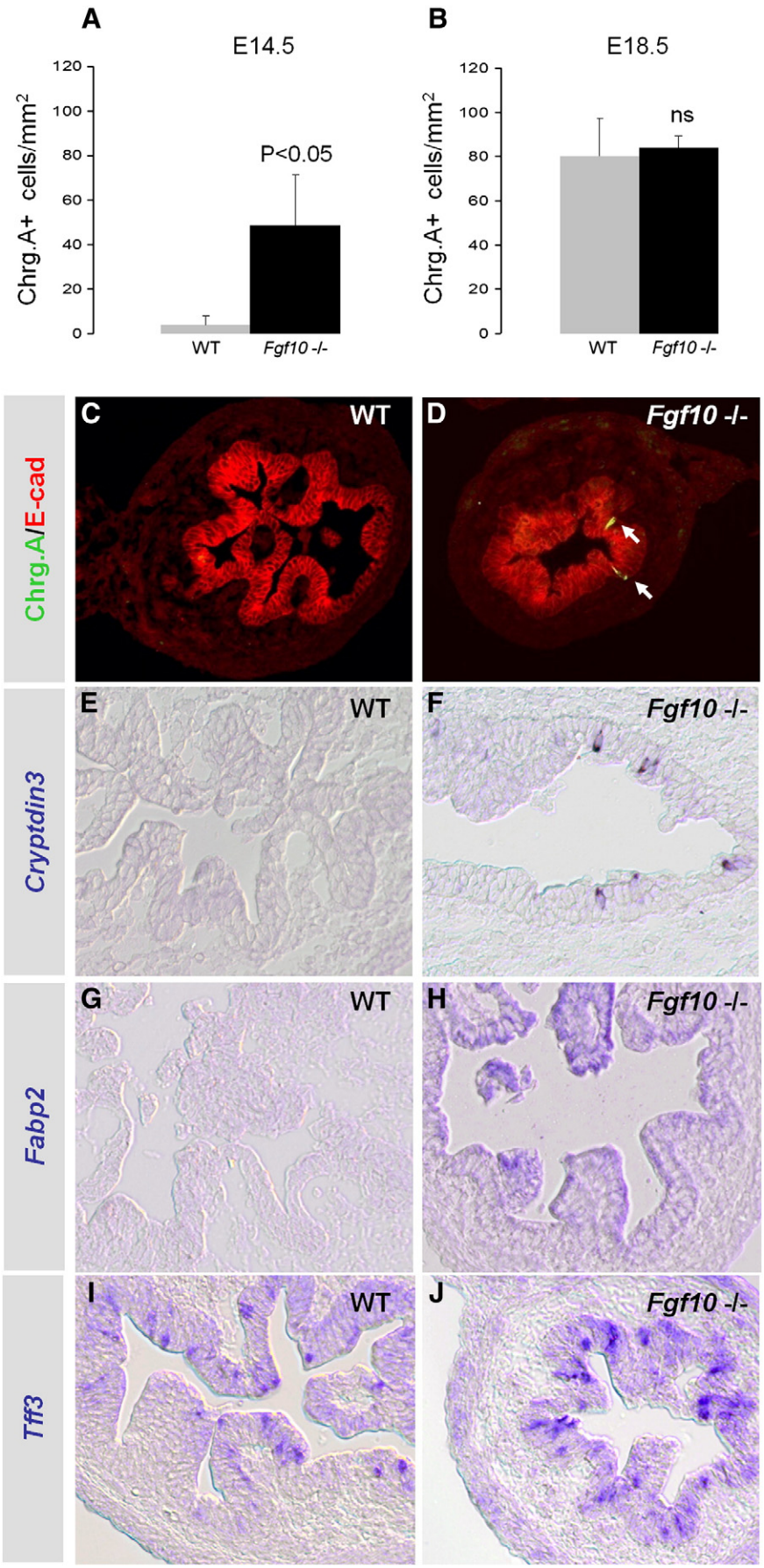
A
E14.5
Chrg.A+ cells/mm2
120
100
80
60
40
20
0
P<0.05
WT
Fgf10 -/-
B
E18.5
ns
C
WT
D
Fgf10 -/-
Chrg.A/E-cad
E
F
Cryptdin3
G
H
Fabp2
I
J
Tff3

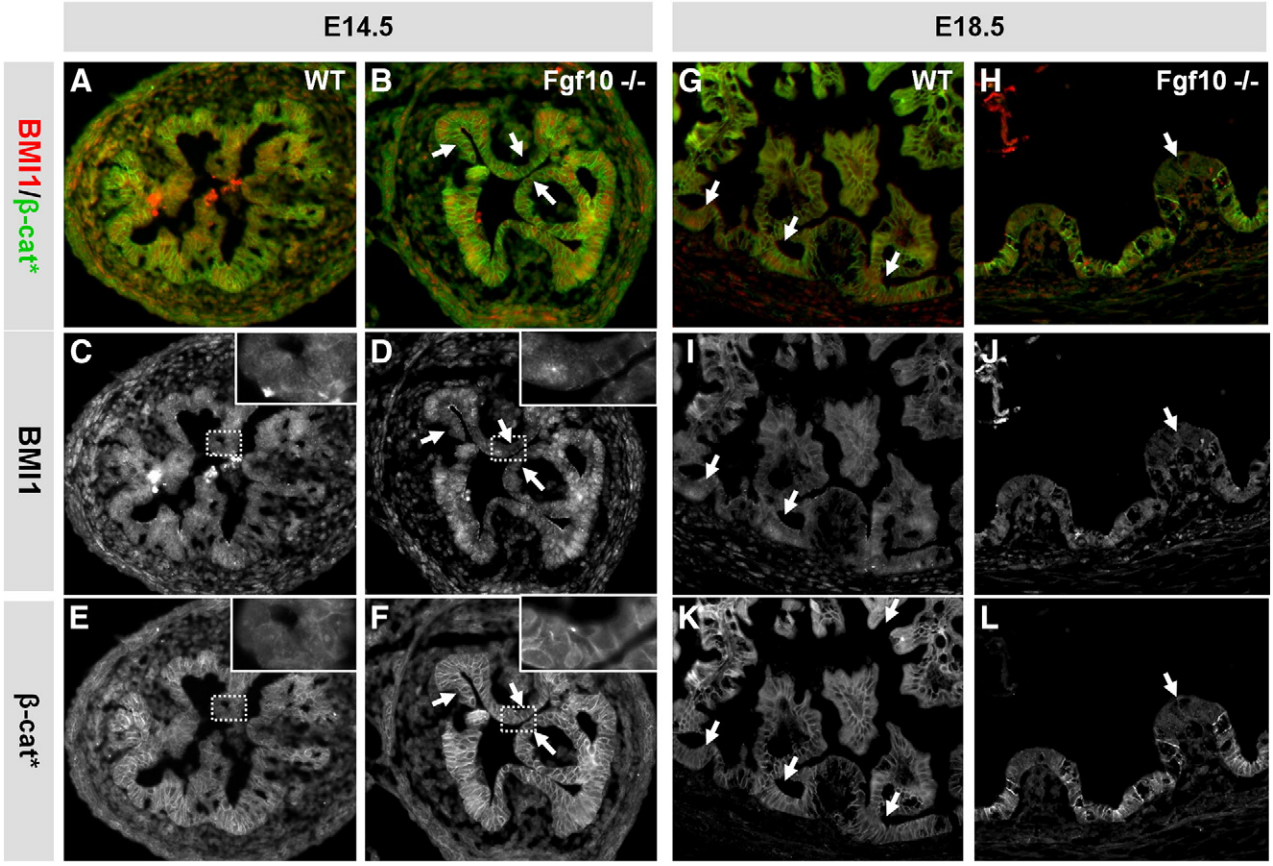

Fig. 9. BMI1 and nuclear β-catenin expression. IHC of *Fgf10*−/− duodenum at E14.5 (A–F) and E18.5 (type I) (G–L) using a BMI1 antibody and an antibody that can detect nuclear β-catenin (β-cat*). A, B, G and H are composite images showing BMI1 and β-catenin expression. C, D, I and J show BMI1 expression. E, F, K and L show β-catenin expression. At E14.5 the entire WT epithelium is strongly BMI1 positive, while there are regions with low BMI1 expression in the FGF10 KO (arrows in B and D). Note how the BMI1 positive cell in the insert in D has nuclear β-catenin expression, while the BMI1 negative cells do not. At E18.5 BMI1 positive cells are exclusively located in the progenitor niche in WT duodenum (arrows in G, I and K). In the FGF10 KO, BMI1 is similarly expressed basally and the rare differentiated villus cells are BMI1 negative (arrows in H, J and L).

data demonstrate that FGF10 overexpression outside the basal domain is sufficient to expand the basal niche and disrupt radial patterning, which strongly suggests that FGF10 secreted from the mesenchyme normally creates a gradient for radial patterning of intrinsic endodermal factors such as *Cdx2* and *Shh*. The fact that the expansion of the basal niche did not lead to an increase in the number of proliferating cells furthermore demonstrates that FGF10 maintains cells in a non-dividing state, resembling enteric stem cells rather than the frequently dividing progenitor cells. Upregulation of the stem cell marker Bmi1 in all epithelial cells strongly supports this notion.

As the expansion of the basal niche was not caused by an increase in the proliferative index or changes in cell survival, we next proceeded to analyze cell differentiation. Our analysis showed that overall differentiation was attenuated, although not completely inhibited by the presence of FGF10. Paneth cells were completely absent, while differentiation of endocrine cells and absorptive enterocytes was markedly attenuated, and goblet cell maturation arrested at an immature stage. Current models support an early divergence of a common secretory precursor cell from the enterocyte precursor and a subsequent divergence into a Paneth/goblet precursor and an endocrine precursor. Since FGF10 has an inhibitory effect on enterocyte differentiation, as well as on secretory cell fates, it is either affecting the common precursor, or affecting both the enterocyte precursor and specific secretory precursor cell stages. The B-class bHLH transcription factor Math1 is required for intestinal secretory cell differentiation (Yang et al., 2001), and is upstream from the zinc finger transcription factor GFI1, which has been shown to affect the choice between a Paneth/goblet fate and an endocrine fate (Shroyer et al., 2005). We see a marked decrease in both Math1$^+$ and GFI1$^+$ cells, demonstrating that very few secretory precursor cells form. We therefore conclude that FGF10 suppress differentiation already at the multipotent stem/progenitor cell stage. Interestingly, the few secretory cells that do bypass the FGF10 inhibitory effect preferentially enter the goblet cell lineage. Immature goblet cells still have potential for mitosis (Karam, 1999;Troughton and Trier, 1969), while Paneth and enteroendocrine cells are non-proliferative. Consequently, the presence of goblet cells may be due to its unique capacity for expansion in the differentiating state, allowing the few cells that escape initial repression to expand.

Investigating putative downstream mechanisms of FGF10 signaling, we find that *Fgf10* overexpression leads to upregulation of FGFR-signaling targets *Sprouty2, Etv4 and Etv5*. Sprouty2 is a feedback inhibitor of FGFR-signaling that exerts its inhibitory effect on RTK-signaling by intercepting elements of the MAP-kinase pathway (Tefft et al., 2002), while ETV4 and ETV5 are transcription factors that mediate FGFR effects downstream of MAP-kinase signaling on target genes in the lung and pancreas (Kobberup et al., 2007;Liu et al., 2003). Based on these results we conclude that the MAP-kinase pathway is activated by FGF10 in the intestine. The observed upregulation of *Etv4* and *Etv5* is particularly interesting, as the Ets factor transcription

Fig. 8. Premature differentiation at E14.5. A: Quantification of ChrgA$^+$ endocrine cells per epithelial (E-cad$^+$) area in E14.5 duodenum showing mean of $n=3$ embryos and SEM. B: Quantification of ChrgA$^+$ cells at E18.5. C,D: IHC of ChrgA and E-cadherin at E14.5. Arrows point to ChrgA$^+$ cells. E, F: ISH of *Cryptdin3*$^+$ Paneth cells at E14.5. G, H: ISH of *Fabp2*$^+$ enterocytes at E14.5. I, J: ISH of *Tff3*$^+$goblet cell precursors at E14.5.

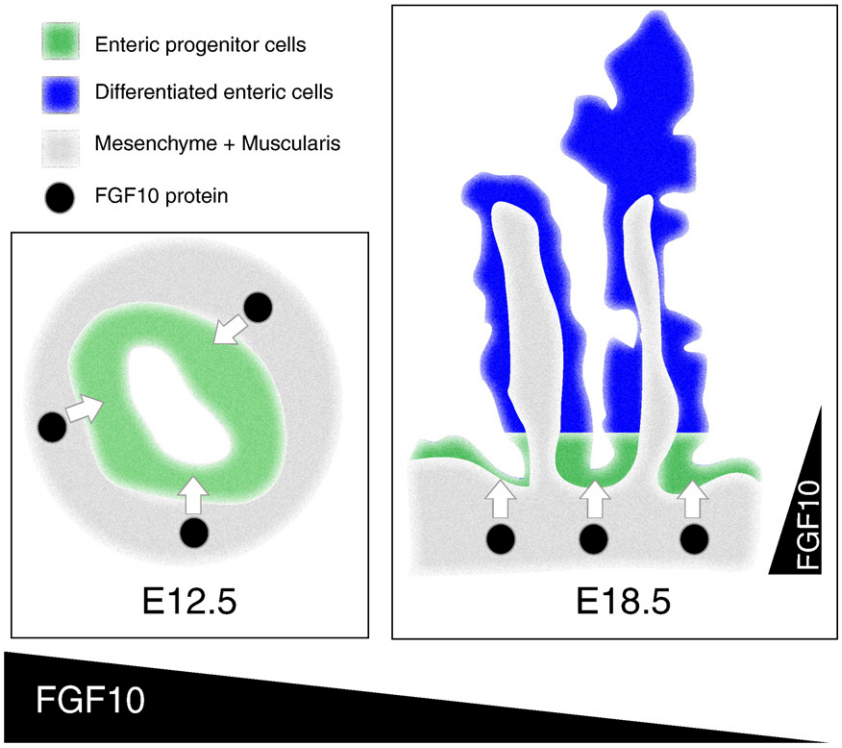

Fig. 10. Model of progenitor cell maintenance in the duodenum. The immature duodenal epithelium at E12.5 (left side of figure) consists of undifferentiated multipotent progenitor cells. At this time, FGF10 is secreted from the mesenchyme at a high level which probably is sufficient to reach all the epithelial cells. The progenitor cells all express the FGF10 receptor FGFR2b and are dependent on mesenchymal FGF10 in order not to differentiate prematurely. At E18.5 (right side of figure), the duodenum has formed crypt–villus units with stem cells and progenitor cells located in the crypt region and differentiated cells located primarily on the villus. The progenitor cells still express FGFR2b, while differentiated cells cease to express the receptor. At this time, FGF10 is secreted at lower levels from basally located mesenchymal cells. This results in a gradient of FGF10 with highest expression in the crypt area. Maintenance of this gradient is necessary in order to restrict the progenitor niche and maintain radial patterning of essential signaling factors such as Cdx2 and Shh. The drawings are graphical representations of H&E stained E12.5 and E18.5 duodenal sections.

family has been implicated in both enteric development and disease. Several Ets factors are expressed in the intestinal epithelium during development (Jedlicka and Gutierrez-Hartmann, 2008), but so far only *Elf3* (E74-like factor-3) KO mice have been shown to have an intestinal phenotype. These mice have impaired villus morphogenesis and enterocyte differentiation (Ng et al., 2002) with some similarity to what we have observed in the FGF10 KO model. The epithelial Ets factors do not seem to have completely overlapping functions in the intestines, as a dominant negative approach targeting all Ets factors in the intestinal epithelium, resulted in a somewhat different phenotype (Jedlicka et al., 2009). *Etv4* KO mice are viable and only have known defects in male sexual function and neuronal development (Laing et al., 2000), and *Etv5* KO mice only have known defects in spermatogonial differentiation (Chen et al., 2005). Etv4 and Etv5 are both members of the PEA3 subfamily and their shared expression domain indicates possible redundancy; it will therefore be interesting to know the intestinal phenotype of the compound *Etv4* and *Etv5* KO, although the early lethality of this mutant (Zhang et al., 2009) makes the analysis dependent on a tissue targeted approach. Ongoing research is currently addressing the roles of ETV4 and ETV5 in more detail.

Hedgehog, Wnt, BMP and Notch signaling also regulate intestinal morphogenesis, and the pathways interact with each other to balance progenitor maintenance and differentiation. We show that *Fgf10* overexpression in the duodenum interferes with Sonic Hedgehog, but we did not find evidence to suggest changes in WNT, BMP or Notch-signaling. *Shh* was upregulated and basal confinement of *Shh* disrupted, but based on our study it is not possible to conclude whether this is a direct effect, or a secondary effect due to expansion of the progenitor cells. Since *Etv4* and *Etv5* have been shown to regulate *Shh* downstream of FGF-signaling in the limb bud (Zhang et al., 2009), it is likely that this direct mechanism is also active during radial patterning of the intestinal epithelium.

Given that gain-of-function of *Fgf10* resulted in a spatial expansion of the stem cell and progenitor niche due to attenuation of cell differentiation, we questioned using a loss-of-function model whether *Fgf10* is required for the temporal maintenance of progenitor cells before terminal differentiation, i.e. when FGF10 levels are high, and found that this is indeed the case. *Fgf10* loss led to premature differentiation of all enteric cell lineages as early as E14.5. Whereas premature differentiation of all enteric cell lineages has not previously been observed, premature differentiation of Paneth cells are also seen in *Hes1* KO (Suzuki et al., 2005) and *Lgr5* KO mice (Garcia et al., 2009). Furthermore, differentiation of Paneth cells and enterocytes has been observed in the progenitor niche of adult enteric cells expressing a constitutively active Rac1 (Stappenbeck and Gordon, 2000). Our observation that loss of FGF10 leads to premature differentiation of all enteric cell lineages as early as E14.5, thus makes it likely that the FGF10 gradient provides the position dependent cue for cellular differentiation (see Fig. 10), upstream from intracellular signaling pathways in the epithelial cell lineages. Whereas we were unable to analyze changes in Lgr5 and Rac1 in this study, we did see a loss of the Wnt signaling target and stem cell marker BMI1 in some epithelial cells at E14.5. These cells also lacked nuclear beta-catenin. We did not observe any changes in HES1 expression in the duodenum after FGF10 loss, although we have previously shown HES1 to be affected by changes in FGF10 levels in the pancreas and stomach.

In accordance with previous studies in the colon and cecum we observed hypotrophy of the duodenal epithelium during later stages, as evidenced by a decreased epithelial area and incomplete maturation with a low number of stunted villi, but in contrast with their findings we did not see any changes in cell proliferation at E14.5, when the

hypotrophy was already starting to manifest, and actually observed a relative increase in cell proliferation at E18.5. This relative increase can however be ascribed to a decrease in villus epithelium, as proliferating cells are found only in the basal epithelium. With regard to cell survival, which aforementioned studies also found affected in the absence of *Fgf10*, we did observe an increase in apoptosis, but not until E18.5, and only in the form of cell shedding, which has so far only been reported as apoptosis of mature cells. We therefore conclude that the stunted duodenal morphogenetic development and possibly also the duodenal atresia observed in *Fgf10*−/− mice is a result of epithelial reduction caused by a loss of progenitor cells due to premature differentiation. We speculate that these premature cells subsequently undergo apoptosis and are shed from the epithelium.

After analyzing the effect of loss and gain of *Fgf10*, we have demonstrated that enteric stem cells and progenitor cells in the early embryonic epithelium are dependent on a mesenchymal signal in the form of FGF10 in order not to differentiate prematurely, and that a morphogen gradient of *Fgf10* with highest expression in the crypt area is necessary in order to restrict the progenitor niche during later development (see Fig. 10). Prior to birth, the levels of FGF10 are negligible, while FGF1 is upregulated, suggesting that this FGFR2b agonist takes over the function of FGF10 postnatally. We conclude that FGF10 is necessary for maintenance of the embryonic enteric progenitor cell population and ectopic FGF10 overexpression is sufficient to prevent cell differentiation in the context of the otherwise normal intestine. This underlying role of *Fgf10* has not previously been revealed in the intestines. This emphasizes the need to inspect all aspects of development and use several different models in order to fully comprehend the function of a signaling molecule. We demonstrate that FGF10 signals through the MAPK pathway and induces BMI1, ETV4 and ETV5 in the duodenum. This result is very interesting in the light of the upregulation of *Fgf10*, *Fgfr2b* (La Rosa et al., 2001;Matsuike et al., 2001), Bmi1 (Kim et al., 2004) and ETV4 (Jedlicka and Gutierrez-Hartmann, 2008) observed in colorectal cancers, pointing to a role of this pathway in both embryogenesis and carcinogenesis.

Supplementary materials related to this article can be found online at doi:10.1016/j.ydbio.2010.09.010.

Acknowledgments

This work was supported by NIH-R01 DK070636 (J.J.) and the American Diabetes Association (Career Development Award, J.J). Further support was obtained from NIH grant number P30 DK57516 (Diabetes and Endocrinology Research Center). PN is supported by the Swedish Research Council. We thank Dr. N. Brown for supplying us with the rabbit α-Hes1 antibody (Lee et al., 2005), Dr. Bellen for the α-Gfi1 antibody (Wallis et al., 2003), Dr. Wright for the goat α-PDX1 antibody, Dr. Sussel for the *Fabp2* plasmid and Dr. McMahon for the *Shh* plasmid. The U. Colorado Cancer Center transgenic facility is thanked for generating the transgenic embryos and Erin West is thanked for technical assistance.

References

Arman, E., Haffner-Krausz, R., Gorivodsky, M., Lonai, P., 1999. Fgfr2 is required for limb outgrowth and lung-branching morphogenesis. Proc. Natl. Acad. Sci. USA 96, 11895–11899.

Bellusci, S., Grindley, J., Emoto, H., Itoh, N., Hogan, B.L., 1997. Fibroblast growth factor 10 (FGF10) and branching morphogenesis in the embryonic mouse lung. Development 124, 4867–4878.

Bhushan, A., Itoh, N., Kato, S., Thiery, J.P., Czernichow, P., Bellusci, S., Scharfmann, R., 2001. Fgf10 is essential for maintaining the proliferative capacity of epithelial progenitor cells during early pancreatic organogenesis. Development 128, 5109–5117.

Boland, C.R., Montgomery, C.K., Kim, Y.S., 1982. Alterations in human colonic mucin occurring with cellular differentiation and malignant transformation. Proc. Natl. Acad. Sci. USA 79, 2051–2055.

Boyer, D.F., Fujitani, Y., Gannon, M., Powers, A.C., Stein, R.W., Wright, C.V., 2006. Complementation rescue of Pdx1 null phenotype demonstrates distinct roles of proximal and distal cis-regulatory sequences in pancreatic and duodenal expression. Dev. Biol. 298, 616–631.

Burns, R.C., Fairbanks, T.J., Sala, F., De Langhe, S., Mailleux, A., Thiery, J.P., Dickson, C., Itoh, N., Warburton, D., Anderson, K.D., Bellusci, S., 2004. Requirement for fibroblast growth factor 10 or fibroblast growth factor receptor 2-IIIb signaling for cecal development in mouse. Dev. Biol. 265, 61–74.

Chen, C., Ouyang, W., Grigura, V., Zhou, Q., Carnes, K., Lim, H., Zhao, G.Q., Arber, S., Kurpios, N., Murphy, T.L., Cheng, A.M., Hassell, J.A., Chandrashekar, V., Hofmann, M.C., Hess, R.A., Murphy, K.M., 2005. ERM is required for transcriptional control of the spermatogonial stem cell niche. Nature 436, 1030–1034.

Desai, S., Loomis, Z., Pugh-Bernard, A., Schrunk, J., Doyle, M.J., Minic, A., McCoy, E., Sussel, L., 2008. Nkx2.2 regulates cell fate choice in the enteroendocrine cell lineages of the intestine. Dev. Biol. 313, 58–66.

Dvorak, P., Dvorakova, D., Koskova, S., Vodinska, M., Najvirtova, M., Krekac, D., Hampl, A., 2005. Expression and potential role of fibroblast growth factor 2 and its receptors in human embryonic stem cells. Stem Cells 23, 1200–1211.

Fairbanks, T.J., Kanard, R.C., De Langhe, S.P., Sala, F.G., Del Moral, P.M., Warburton, D., Anderson, K.D., Bellusci, S., Burns, R.C., 2004. A genetic mechanism for cecal atresia: the role of the Fgf10 signaling pathway. J. Surg. Res. 120, 201–209.

Fairbanks, T.J., Kanard, R.C., Del Moral, P.M., Sala, F.G., De Langhe, S.P., Lopez, C.A., Veltmaat, J.M., Warburton, D., Anderson, K.D., Bellusci, S., Burns, R.C., 2005. Colonic atresia without mesenteric vascular occlusion. The role of the fibroblast growth factor 10 signaling pathway. J. Pediatr. Surg. 40, 390–396.

Fre, S., Huyghe, M., Mourikis, P., Robine, S., Louvard, D., Artavanis-Tsakonas, S., 2005. Notch signals control the fate of immature progenitor cells in the intestine. Nature 435, 964–968.

Garcia, M.I., Ghiani, M., Lefort, A., Libert, F., Strollo, S., Vassart, G., 2009. LGR5 deficiency deregulates Wnt signaling and leads to precocious Paneth cell differentiation in the fetal intestine. Dev. Biol. 331, 58–67.

Haffen, K., Kedinger, M., Simon-Assmann, P., 1987. Mesenchyme-dependent differentiation of epithelial progenitor cells in the gut. J. Pediatr. Gastroenterol. Nutr. 6, 14–23.

Hart, A., Papadopoulou, S., Edlund, H., 2003. Fgf10 maintains notch activation, stimulates proliferation, and blocks differentiation of pancreatic epithelial cells. Dev. Dyn. 228, 185–193.

He, X.C., Zhang, J., Tong, W.G., Tawfik, O., Ross, J., Scoville, D.H., Tian, Q., Zeng, X., He, X., Wiedemann, L.M., Mishina, Y., Li, L., 2004. BMP signaling inhibits intestinal stem cell self-renewal through suppression of Wnt-beta-catenin signaling. Nat. Genet. 36, 1117–1121.

Jedlicka, P., Gutierrez-Hartmann, A., 2008. Ets transcription factors in intestinal morphogenesis, homeostasis and disease. Histol. Histopathol. 23, 1417–1424.

Jedlicka, P., Sui, X., Sussel, L., Gutierrez-Hartmann, A., 2009. Ets transcription factors control epithelial maturation and transit and crypt–villus morphogenesis in the mammalian intestine. Am. J. Pathol. 174, 1280–1290.

Jensen, J., Serup, P., Karlsen, C., Nielsen, T.F., Madsen, O.D., 1996. mRNA profiling of rat islet tumors reveals nkx 6.1 as a beta-cell-specific homeodomain transcription factor. J. Biol. Chem. 271, 18749–18758.

Jensen, J., Pedersen, E.E., Galante, P., Hald, J., Heller, R.S., Ishibashi, M., Kageyama, R., Guillemot, F., Serup, P., Madsen, O.D., 2000. Control of endodermal endocrine development by Hes-1. Nat. Genet. 24, 36–44.

Kanard, R.C., Fairbanks, T.J., De Langhe, S.P., Sala, F.G., Del Moral, P.M., Lopez, C.A., Warburton, D., Anderson, K.D., Bellusci, S., Burns, R.C., 2005. Fibroblast growth factor-10 serves a regulatory role in duodenal development. J. Pediatr. Surg. 40, 313–316.

Karam, S.M., 1999. Lineage commitment and maturation of epithelial cells in the gut. Front. Biosci. 4, D286–D298.

Kedinger, M., Simon-Assmann, P., Haffen, K., 1987. Growth and differentiation of intestinal endodermal cells in a coculture system. Gut 28 (Suppl), 237–241.

Kim, J.H., Yoon, S.Y., Kim, C.N., Joo, J.H., Moon, S.K., Choe, I.S., Choe, Y.K., Kim, J.W., 2004. The Bmi-1 oncoprotein is overexpressed in human colorectal cancer and correlates with the reduced p16INK4a/p14ARF proteins. Cancer Lett. 203, 217–224.

Kobberup, S., Nyeng, P., Juhl, K., Hutton, J., Jensen, J., 2007. ETS-family genes in pancreatic development. Dev. Dyn. 236, 3100–3110.

Korinek, V., Barker, N., Moerer, P., van, D.E., Huls, G., Peters, P.J., Clevers, H., 1998. Depletion of epithelial stem-cell compartments in the small intestine of mice lacking Tcf-4. Nat. Genet. 19, 379–383.

Kruger, V., Khoshvaghti, M., Reutter, H., Vogt, H., Boemers, T.M., Ludwig, M., 2008. Investigation of FGF10 as a candidate gene in patients with anorectal malformations and exstrophy of the cloaca. Pediatr. Surg. Int. 24, 893–897.

La Rosa, S., Uccella, S., Erba, S., Capella, C., Sessa, F., 2001. Immunohistochemical detection of fibroblast growth factor receptors in normal endocrine cells and related tumors of the digestive system. Appl. Immunohistochem. Mol. Morphol. 9, 319–328.

Laing, M.A., Coonrod, S., Hinton, B.T., Downie, J.W., Tozer, R., Rudnicki, M.A., Hassell, J.A., 2000. Male sexual dysfunction in mice bearing targeted mutant alleles of the PEA3 ets gene. Mol. Cell. Biol. 20, 9337–9345.

Lee, H.Y., Wroblewski, E., Philips, G.T., Stair, C.N., Conley, K., Reedy, M., Mastick, G.S., Brown, N.L., 2005. Multiple requirements for Hes 1 during early eye formation. Dev. Biol. 284, 464–478.

Liu, Y., Jiang, H., Crawford, H.C., Hogan, B.L., 2003. Role for ETS domain transcription factors Pea3/Erm in mouse lung development. Dev. Biol. 261, 10–24.

Madison, B.B., Braunstein, K., Kuizon, E., Portman, K., Qiao, X.T., Gumucio, D.L., 2005. Epithelial hedgehog signals pattern the intestinal crypt–villus axis. Development 132, 279–289.

Matsuike, A., Ishiwata, T., Watanabe, M., Asano, G., 2001. Expression of fibroblast growth factor (FGF)-10 in human colorectal adenocarcinoma cells. J. Nippon Med. Sch. 68, 397–404.

Min, H., Danilenko, D.M., Scully, S.A., Bolon, B., Ring, B.D., Tarpley, J.E., DeRose, M., Simonet, W.S., 1998. Fgf-10 is required for both limb and lung development and exhibits striking functional similarity to Drosophila branchless. Genes Dev. 12, 3156–3161.

Minowada, G., Jarvis, L.A., Chi, C.L., Neubuser, A., Sun, X., Hacohen, N., Krasnow, M.A., Martin, G.R., 1999. Vertebrate Sprouty genes are induced by FGF signaling and can cause chondrodysplasia when overexpressed. Development 126, 4465–4475.

Miyamoto, T., Leconte, I., Swain, J.L., Fox, J.C., 1998. Autocrine FGF signaling is required for vascular smooth muscle cell survival in vitro. J. Cell. Physiol. 177, 58–67.

Ng, A.Y., Waring, P., Ristevski, S., Wang, C., Wilson, T., Pritchard, M., Hertzog, P., Kola, I., 2002. Inactivation of the transcription factor Elf3 in mice results in dysmorphogenesis and altered differentiation of intestinal epithelium. Gastroenterology 122, 1455–1466.

Norgaard, G.A., Jensen, J.N., Jensen, J., 2003. FGF10 signaling maintains the pancreatic progenitor cell state revealing a novel role of Notch in organ development. Dev. Biol. 264, 323–338.

Nyeng, P., Norgaard, G.A., Kobberup, S., Jensen, J., 2007. FGF10 signaling controls stomach morphogenesis. Dev. Biol. 303, 295–310.

Ohlsson, H., Karlsson, K., Edlund, T., 1993. IPF1, a homeodomain-containing transactivator of the insulin gene. EMBO J. 12, 4251–4259.

Pinto, D., Gregorieff, A., Begthel, H., Clevers, H., 2003. Canonical Wnt signals are essential for homeostasis of the intestinal epithelium. Genes Dev. 17, 1709–1713.

Powers, C.J., McLeskey, S.W., Wellstein, A., 2000. Fibroblast growth factors, their receptors and signaling. Endocr. Relat. Cancer 7, 165–197.

Pulkkinen, M.A., Spencer-Dene, B., Dickson, C., Otonkoski, T., 2003. The IIIb isoform of fibroblast growth factor receptor 2 is required for proper growth and branching of pancreatic ductal epithelium but not for differentiation of exocrine or endocrine cells. Mech. Dev. 120, 167–175.

Ramalho-Santos, M., Melton, D.A., McMahon, A.P., 2000. Hedgehog signals regulate multiple aspects of gastrointestinal development. Development 127, 2763–2772.

Sala, F.G., Curtis, J.L., Veltmaat, J.M., Del Moral, P.M., Le, L.T., Fairbanks, T.J., Warburton, D., Ford, H., Wang, K., Burns, R.C., Bellusci, S., 2006. Fibroblast growth factor 10 is required for survival and proliferation but not differentiation of intestinal epithelial progenitor cells during murine colon development. Dev. Biol. 299, 373–385.

Sangiorgi, E., Capecchi, M.R., 2008. Bmi1 is expressed in vivo in intestinal stem cells. Nat. Genet. 40, 915–920.

Sekine, K., Ohuchi, H., Fujiwara, M., Yamasaki, M., Yoshizawa, T., Sato, T., Yagishita, N., Matsui, D., Koga, Y., Itoh, N., Kato, S., 1999. Fgf10 is essential for limb and lung formation. Nat. Genet. 21, 138–141.

Shroyer, N.F., Wallis, D., Venken, K.J., Bellen, H.J., Zoghbi, H.Y., 2005. Gfi1 functions downstream of Math1 to control intestinal secretory cell subtype allocation and differentiation. Genes Dev. 19, 2412–2417.

Spencer-Dene, B., Sala, F.G., Bellusci, S., Gschmeissner, S., Stamp, G., Dickson, C., 2006. Stomach development is dependent on fibroblast growth factor 10/fibroblast growth factor receptor 2b-mediated signaling. Gastroenterology 130, 1233–1244.

Stappenbeck, T.S., Gordon, J.I., 2000. Rac1 mutations produce aberrant epithelial differentiation in the developing and adult mouse small intestine. Development 127, 2629–2642.

Suzuki, K., Fukui, H., Kayahara, T., Sawada, M., Seno, H., Hiai, H., Kageyama, R., Okano, H., Chiba, T., 2005. Hes1-deficient mice show precocious differentiation of Paneth cells in the small intestine. Biochem. Biophys. Res. Commun. 328, 348–352.

Tatekawa, Y., Kanehiro, H., Nakajima, Y., 2007. Duodenal atresia associated with "apple peel" small bowel without deletion of fibroblast growth factor-10 or fibroblast growth factor receptor 2IIIb: report of a case. Surg. Today 37, 430–433.

Tefft, D., Lee, M., Smith, S., Crowe, D.L., Bellusci, S., Warburton, D., 2002. mSprouty2 inhibits FGF10-activated MAP kinase by differentially binding to upstream target proteins. Am. J. Physiol. Lung Cell. Mol. Physiol. 283, L700–L706.

Troughton, W.D., Trier, J.S., 1969. Paneth and goblet cell renewal in mouse duodenal crypts. J. Cell Biol. 41, 251–268.

van Es, J.H., van Gijn, M.E., Riccio, O., van den, B.M., Vooijs, M., Begthel, H., Cozijnsen, M., Robine, S., Winton, D.J., Radtke, F., Clevers, H., 2005. Notch/gamma-secretase inhibition turns proliferative cells in intestinal crypts and adenomas into goblet cells. Nature 435, 959–963.

Visel, A., Thaller, C., Eichele, G., 2004. GenePaint.org: an atlas of gene expression patterns in the mouse embryo. Nucleic Acids Res. 32, D552–D556.

Wallis, D., Hamblen, M., Zhou, Y., Venken, K.J., Schumacher, A., Grimes, H.L., Zoghbi, H.Y., Orkin, S.H., Bellen, H.J., 2003. The zinc finger transcription factor Gfi1, implicated in lymphomagenesis, is required for inner ear hair cell differentiation and survival. Development 130, 221–232.

Wong, G.T., Manfra, D., Poulet, F.M., Zhang, Q., Josien, H., Bara, T., Engstrom, L., Pinzon-Ortiz, M., Fine, J.S., Lee, H.J., Zhang, L., Higgins, G.A., Parker, E.M., 2004. Chronic treatment with the gamma-secretase inhibitor LY-411, 575 inhibits beta-amyloid peptide production and alters lymphopoiesis and intestinal cell differentiation. J. Biol. Chem. 279, 12876–12882.

Wurster, K., Peschke, P., Kuhlmann, W.D., 1983. Cellular localization of lectin-affinity in tissue sections of normal human duodenum. Virchows Arch. A Pathol. Anat. Histopathol. 402, 1–9.

Yang, Q., Bermingham, N.A., Finegold, M.J., Zoghbi, H.Y., 2001. Requirement of Math1 for secretory cell lineage commitment in the mouse intestine. Science 294, 2155–2158.

Zhang, X., Ibrahimi, O.A., Olsen, S.K., Umemori, H., Mohammadi, M., Ornitz, D.M., 2006. Receptor specificity of the fibroblast growth factor family. The complete mammalian FGF family. J. Biol. Chem. 281, 15694–15700.

Zhang, Z., Verheyden, J.M., Hassell, J.A., Sun, X., 2009. FGF-regulated Etv genes are essential for repressing Shh expression in mouse limb buds. Dev. Cell 16, 607–613.